

Effect of Mechanical Alloying and Sintering on Ni-Ti Powders

S. K. Sadrnezhaad* and A. R. Selahi

Department of Materials Science and Engineering,
Sharif University of Technology, Tehran, Iran

ABSTRACT

Commercially pure nickel-titanium powders were mechanically milled in a vertical attritor mill under protective atmosphere for various times from 10 to 24 hr. Products were then compacted and sintered at different temperatures for different times. Amorphization and interatomic phase formation were determined by X-ray diffractometry, scanning electron microscopy and differential scanning calorimetry. Porosity, virtual density, transition temperatures and the amount of Ni₃Ti first increased and then decreased with the milling time. Presence of oxygen in the milling atmosphere showed partial crystallization of NiTi intermetallic compound accompanied with titanium oxide formation.

Key Words: Mechanical alloying; Ni-Ti; Powder; Amorphization; Intermetallic compounds; Sintering; Nitinol; Milling.

*Correspondence: S. K. Sadrnezhaad, Ph. D., Department of Materials Science and Engineering, Sharif University of Technology, Tehran, 11365, Iran; Fax: +9821-6005717; E-mail: sadrnezh@sharif.edu or sarnezh@yahoo.com.

1. INTRODUCTION

Mechanical alloying was first developed by Benjamin and Volin in 1974.^[1] It served as a means of combining the advantages of gamma prime precipitation hardening for intermediate strength and oxide dispersion strengthening in a nickel-base high temperature super alloy. This was also used by Batezzati et al.^[2] in 1988 to prepare mechanically alloyed Ni-Ti powders. Mechanical alloying is now known as an alternative way for production of nanocrystalline intermetallic materials.^[3,4]

It is well known that, besides the three stable intermetallic phases (NiTi₂, NiTi, and Ni₃Ti), several other metastable phases can form during solidification of Ni-Ti equiatomic alloy.^[5] Ageing supersaturated Ni-rich alloy can cause the segregation of Ni₄Ti₃ and Ni₃Ti₂ phases before the formation of Ni₃Ti,^[6-9] whereas NiTi—whose high-temperature crystal structure is B2 (CsCl type) with a lattice parameter of about 0.3 nm—reveals the shape memory effect generally referred to as SME. Annealing followed by cold working and aging can result in formation of a rhombohedral phase before martensitic transformation.^[10,11]

The SME is a thermoelastic process that can be induced by cooling of the B2 phase to a temperature below Ms or by application of an externally applied stress.^[12,13] During cooling, the so-called parent phase undergoes a diffusionless transformation to a martensitic product with a triclinic distortion of the B19 type^[14] lattice or a monoclinic type^[15,16] crystal structure. In Ni-rich alloys, the Ni₄Ti₃ precipitate is the closest phase that can induce memory effect.^[8,11] This can be achieved by annealing of the alloy at 500°C or less.^[17-19]

Although considerable achievements have been obtained on Ni-Ti Shape memory alloy (SMA) during past years, there are still controversies on how to precisely control the SMA characteristics.^[20] An important issue is the choice of alternative production methods as they affect the chemical homogeneity, the porosity, and the contaminants added to the melt. It is, therefore, agreed upon that, although the conventional methods like electric arc melting, vacuum induction melting or combustion synthesis^[21] are suitable for production of Ni-Ti alloys, powder metallurgy must also be considered as a beneficial way of production of the near-net-shape, fine-grain material that can be applicable to the aerospace, automotive, or biomedical industry.^[22]

The formation of B2 phase in NiTi is very sensitive to the chemical composition of the alloy. Melting methods have shortcomings due to (1) gas absorption, (2) elemental vaporization, (3) segregate formation, and (4) crucible contaminate absorption.^[23]

New powder-metallurgical techniques such as self-propagation high-temperature synthesis, liquid-phase sintering, explosive shock wave compression, and mechanical alloying have more recently been reported for production of NiTi from pure elemental powders of nickel and titanium.^[23-27] Each method has its own advantages, disadvantages and need to further development.

Mechanical alloying is a complex process comprised of fragmentation, deformation, cold welding, and short range diffusion occurring within a layer of powder particles trapped between surfaces of two colliding balls.^[28] These events occur in a high-energy ball mill, which is usually one of four common devices. One is a vertical ball mill, such as attritor mill, in which the balls and the metal powders

are charged into a stationary vertical tank and are agitated by impellers radiating from a central rotating shaft.^[28,29] A Second configuration is the vibratory mill exemplified by the SPEX shaker mill. The third is a conventional horizontal ball mill,^[29] and the last is the planetary ball mill.

In this study, a modified attritor mill and a planetary ball mill were used for mechanical alloying of the Ni-Ti powders. The products were then compacted and sintered to make disklike tablets. The properties of the tablets were determined and compared with those produced via other alternative routes.

2. EXPERIMENTAL PROCEDURE

Commercially pure powders of Ni (99.9%) with an average particle size of about 5 μm and Ti (99.9%) with an average particle size of about 30 μm were mixed equiatomically and milled in a vertical attritor mill working with chromium steel balls of either 7.5 or 4.8 mm diameters. To increase the efficiency of the process, the dead zone usually formed at the bottom of the mill^[29,30] was eliminated by addition of an extra impeller to the end of the shaft.^[31] The milling process continued for up to 24 hr at two rotational speeds of 350 and 710 rpm under argon atmosphere.

Ten grams of mixed powders were first milled in separate stages, and X-ray samples were taken at the end of each stage. During milling, the materials were kept cold by holding the external surface of the container isothermal so that the nonisothermal processes could be avoided. Twenty-two grams of a similar powder were then poured into the vial and milled for another 10 hr separated into five 2-hr intervals. An X-ray map was taken after 20 hr of the final product. In a separate experiment, 20 g of mixed powders were milled at the same conditions but with a higher milling rate. The samples were characterized by cobalt radiation ($\lambda = 1.7903 \text{ \AA}$) of a Philips diffractometer.

The mechanically alloyed powders were compacted at 500 MPa using a single action press in a floating die and then annealed at 1000°C for 4 hr. Their virtual density was measured by means of floatation method, and an image analyzer determined their porosity. The cross-section of the samples was metallographically analyzed and their matrix composition was determined by Electron Probe Micro-Analyzer (EPMA). The transition temperatures of the samples were measured by a differential scanning calorimetry (DSC) analyzer, which heated the samples up to 200°C and cooled them down to the room temperature with a heating/cooling rate of 5°C per minute.

3. Results and Discussion

Figure 1 illustrates the micrographs of the pure powders used in these studies. Figure 2 shows the dot map patterns of a typical particle from within a sample that was milled for 20 hr. The distribution of nickel and titanium in the particle is a measure of the progress of the alloying process. A rough estimation implies that the particle consists of around 35 to 40 % nickel and 60 to 65 % titanium, indicating that the diffusion process has partially occurred due to the milling operation.

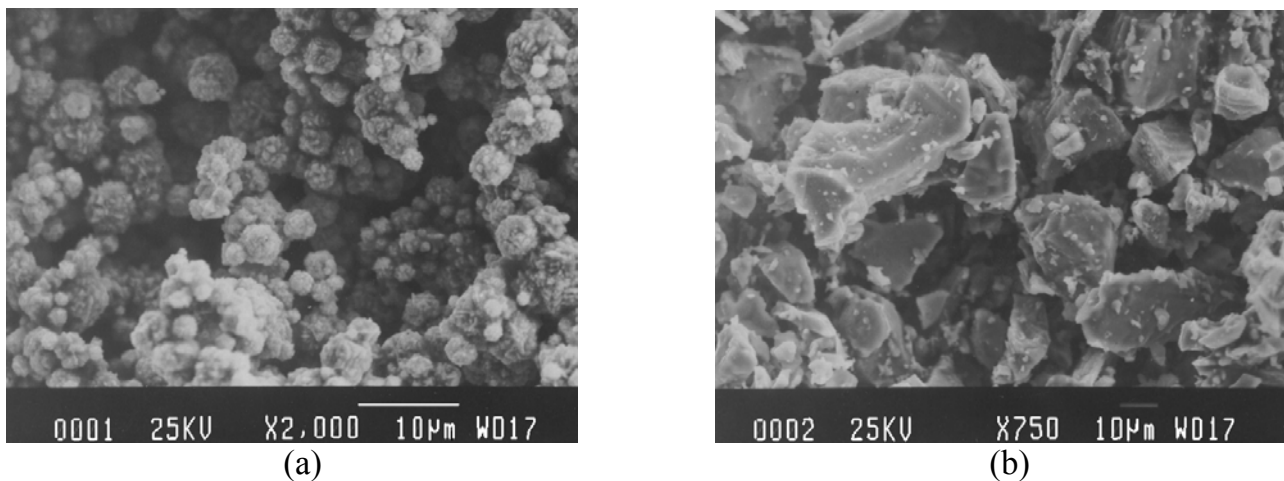


Figure 1. Micrographs of pure powders used to make samples: (a) Ni and (b) Ti. (View this art in color at www.dekker.com.)

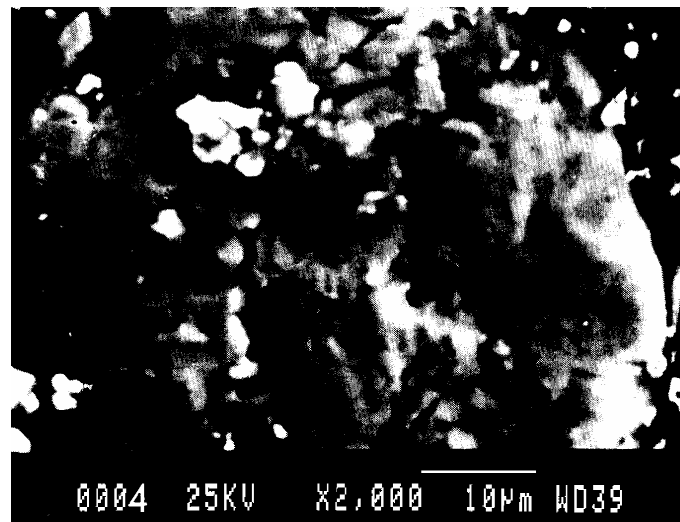
Both grain boundary and volume diffusion can be responsible for the alloying process. It has been proven earlier that the formation of high diffusivity paths, such as dislocations during mechanical alloying, increases the rate of inter-diffusion of the alloying elements.^[32] Observations show that the amounts of the diffused materials will increase by further milling of the sample. An increase in the milling speed, as well as the ball to powder ratio, up to 10:1 will also increase the diffusion rate.

X-ray diffraction (XRD) patterns indicate a typical broad peak of the amorphous phase that appears after 10 hr of milling at 350 rpm (Fig. 3). The reason for interchange of the principal titanium peaks after 8 hr of milling, which is observable in Fig. 3 is not clear to us. A probable cause might be the formation of preferred orientations due to cold working and fracturing of the titanium grains accompanying the accumulation of the dislocations during milling.

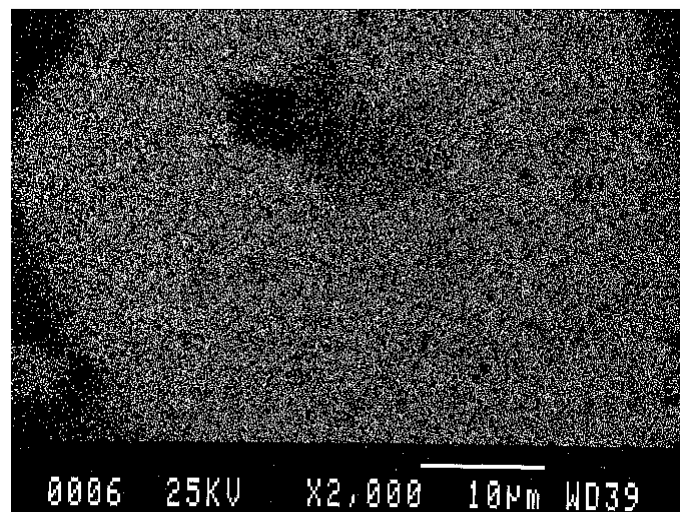
Figure 4 clearly indicates the formation of B19' (martensite) phase from B2 (austenite) in the sintered samples. Table 1 summarizes the transition temperatures of the samples measured after sintering. It is shown that an increase of around 40°C in the transition temperatures occurs due to up to 16 hr milling, whereas about 20°C decrease occurs due to an additional 2 hr milling. These changes are consistent with the ones obtained from comparison of the peaks depicted in Fig. 4.

To understand the reason, one should notice the effect of grain size on stability of the martensite phase. According to the previous investigations, as the grain size decreases, martensite will form easier and would thus be in a more stable condition.^[33] Refinement of the grain size causes, therefore, increasing of the transition temperatures. Further milling, however, results in storage of an excess energy in the powders. This causes the decreasing of the virtual temperatures existing for recovery, recrystallization, and grain growth, resulting in reduction of the transformation temperatures illustrated in Table 1. Every mechanism that has a stronger effect causes a greater change in the transformation temperatures of the samples.

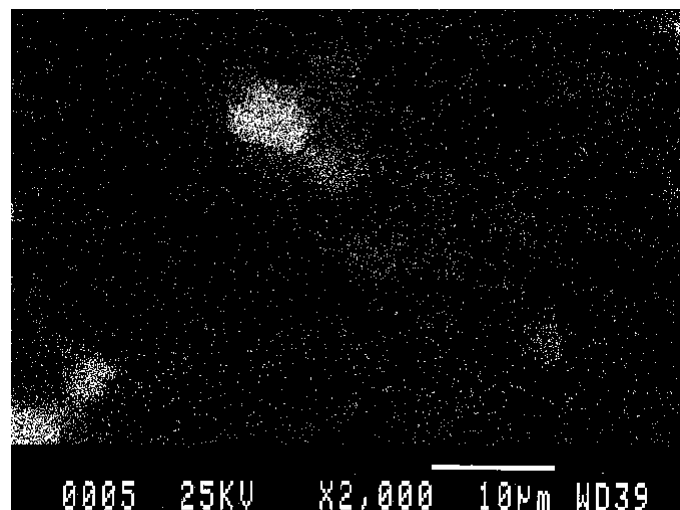
Figure 5 shows the variation of the density of the sintered samples with the milling time. As is seen, the density increases with the milling time. This is due to the negative molar volume change for formation of TiNi from its pure constituents:



a



b



c

Figure 2. X-ray maps of a typical powder particle milled for 20 hr: (a) a powder particle, (b) distribution of Ti inside the particle, and (c) distribution of Ni inside the particle.

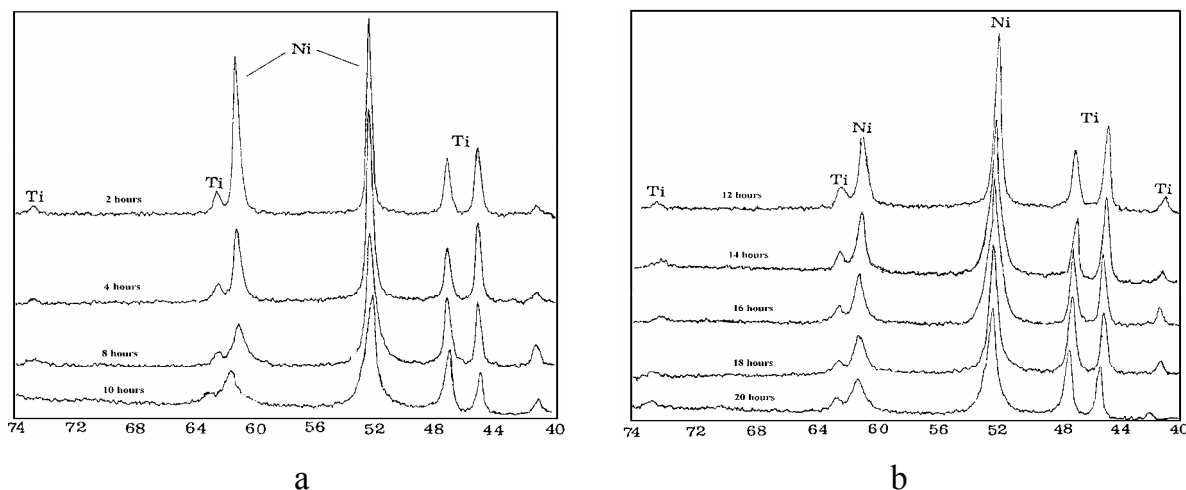


Figure 3. XRD patterns for Ni-Ti mixture after milling in argon for (a) 2, 4, 6, 8 and 10 hr and (b) 12, 14, 16, 18, and 20 hr.

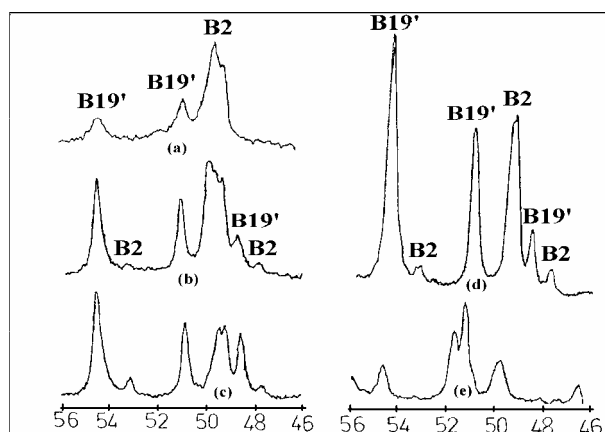


Figure 4. XRD patterns of sintered Ni-Ti powders milled in argon gas for (a) 12, (b) 14, (c) 16, (d) 18, and (e) 20 hr.

Table 1. Effect of milling time on the transition temperatures of the samples made by sintering of the mechanically alloyed powders.

Milling Time (hr)	A_s (°C)	A_f (°C)	M_s (°C)	M_f (°C)
12	106.5	129	119	100
14	142.5	164	148	126
16	152.0	164	150	142
18	130.0	146	135	121

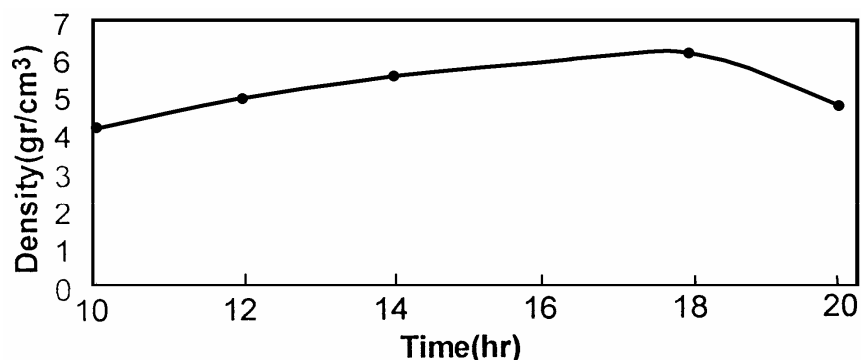


Figure 5. The change of density with the milling time.

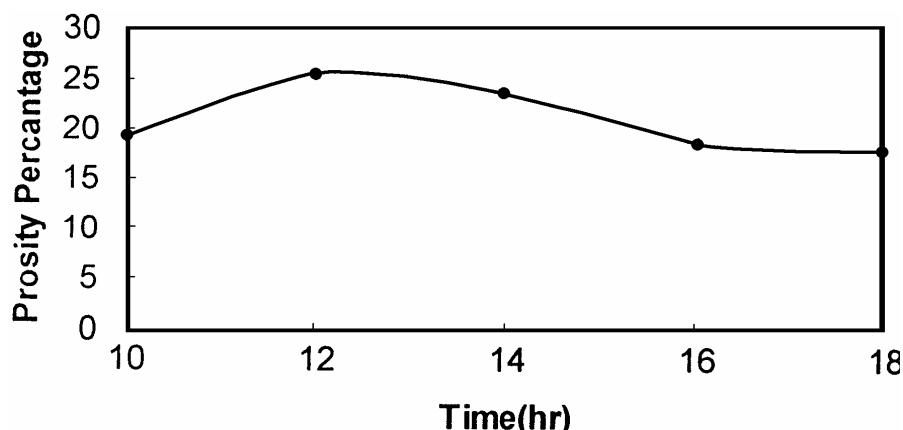


Figure 6. The change of porosity of the sintered sample with the milling time.

$$\Delta V_{\text{NiTi}} = -0.71 \text{ cm}^3/\text{mol}$$

Figure 5 indicates that after milling for 18 hr, the density of the specimen starts to decrease. The reason for this decreasing effect is not obvious to us, but its occurrence is assessed with further experiments. Chemical reactions accompanied by exchange of different phases of highly reactive unstable nature during prolonged mechanical alloying may be responsible for this effect.

Variation of the porosity of the sintered sample with the milling time, shown in Fig. 6, indicates an unusual trend between 10 and 12 hr. It first increases and then decreases with the milling time. To understand the reason, one can pay attention to the major sources of porosity in the sample:

- Initial porosity of the specimen before sintering.^[34]
- Porosities produced due to the faster diffusion of nickel in titanium.^[35]
- Shrinkage pores that form because of the solidification of the liquid phase formed during sintering.^[36]
- Expansion, which occurs because of the internal combustion of Ni with Ti to form NiTi during sintering.^[37]

Mechanical alloying, of course, reduced the effects of the second and the fourth source by application of the milling energy to the specimens. The presence of oxygen,

even at the smallest level, in the milling atmosphere showed, however, that partial crystallization of the NiTi intermetallic compound was accompanied by titanium oxide formation. Gas absorption, partial oxidation, and clustering of the powders were accompanied with great amounts of heat evolution. This heat was constantly removed to keep the initial isothermal milling conditions.

Figure 7 shows the microstructure of the sintered specimens containing two kinds of precipitates: (1) one with a round-shaped edge, and (2) another with a sharp-edged shape. The chemical analyses of both kinds and the matrix were

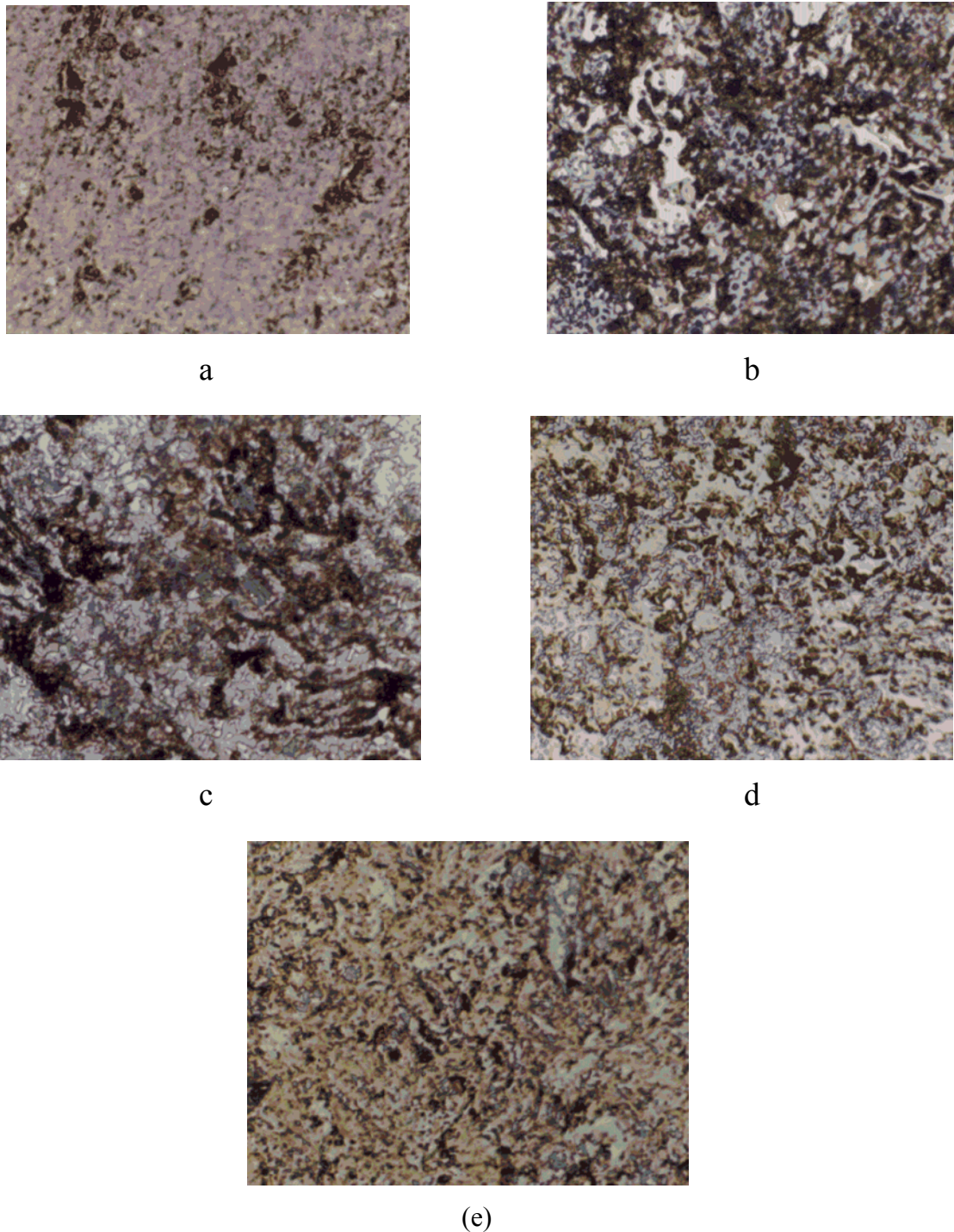
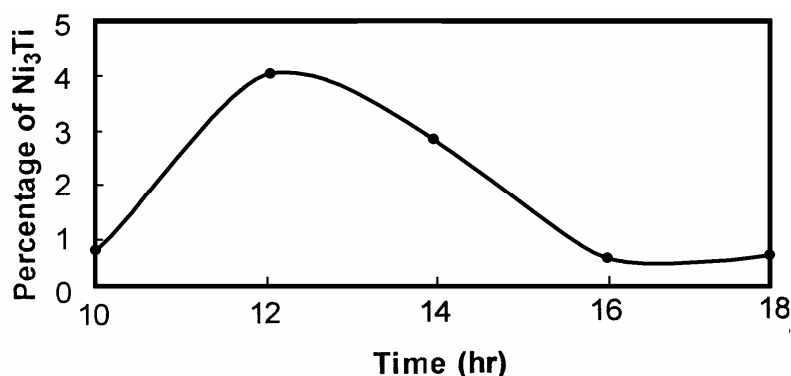
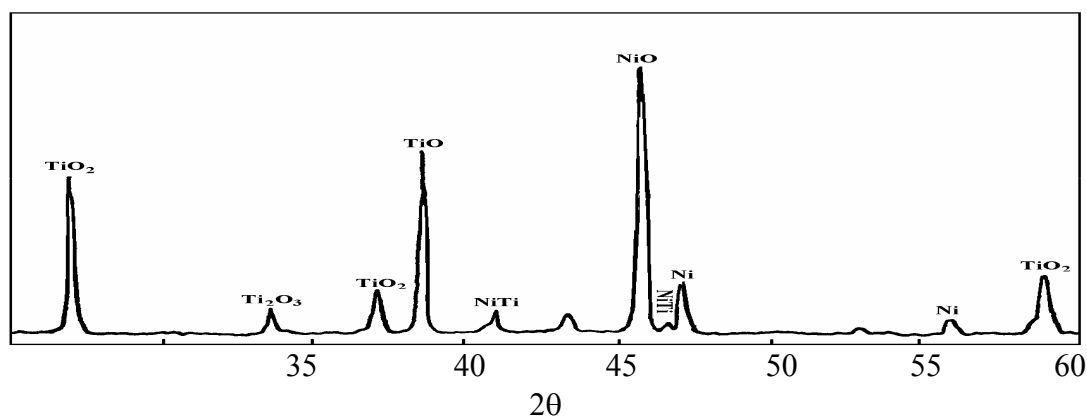


Figure 7. Microstructure of samples made of powders milled for (a) 10 hr, (b) 12 hr, (c) 14 hr, (d) 16 hr, and (e) 18 hr. (View this art in color at www.dekker.com.)

Table 2. Chemical composition of precipitates and the matrix in a sintered specimen.

Shape	Ni atom%	Ti atom%	Compound
Sharp Edge	75.60	27.20	Ni ₃ Ti
Round	57.76	42.57	Ni ₃ Ti ₂
Matrix	49.36	50.69	NiTi

**Figure 8.** Variation of the amount of unstable precipitate Ni₃Ti with the milling time.**Figure 9.** XRD pattern of Ni-Ti mixture milled for 24 hr under atmosphere and then annealed for 1 hr at 920 °C under purified argon.

determined by EPMA. The results indicated the formation of two compounds; Ni₃Ti and Ni₃Ti₂ (Table 2); both being considered as common precipitates in the NiTi alloying process. It was seen that the milling time changed the amount of the intermetallic phases (Fig. 8), but the amount of Ni₃Ti₂ was so small that it could not be measured with image analyzer.

Figure 8 shows that the amount of the intermetallic compound Ni₃Ti increases with the milling time to a maximum value of about 4% that occurs at $t = 12$ hr. This quantity then decreases to values lower than 0.5%, with the milling time exceeding 16 hr. Difference in the diffusion coefficients of the nickel and titanium atoms, as well as their particle size, seems to be responsible for these changes. Further, interatomic diffusion of the constituent elements allows the mixture to approach the

stoichiometric NiTi chemical composition and results in reduction of the amount of the metastable Ni₃Ti phase. Sintering will also affect the change of the composition of Ni₃Ti towards NiTi. Small amount of meta-stable compound Ni₃Ti₂ can also form in the samples milled especially for lower periods (10-12 hr). The presence of the Ni₃Ti and Ni₃Ti₂ compounds has adverse effects on high-temperature workability of the specimens,^[38] and their elimination would improve the hot rolling characteristics of the mechanically alloyed specimens.

Experimental studies showed that the milling under atmosphere resulted in the formation of TiO, Ti₂O₃, and TiO₂ phases; whereas TiO and Ti₂O₃ were unstable and diminished with the milling time. Enthalpies of the oxidation reactions facilitated the formation of the intermetallic NiTi crystalline compound. Figure 9 illustrates the relative amounts of the phases produced after 24 hr milling under atmospheric conditions followed by 1 hr annealing at 920°C under purified argon.

4. CONCLUSIONS

1. The amounts of amorphization and diffusion are functions of the milling time, milling speed, and the charge ratio.
2. The porosity percentage will decrease with increasing of the milling time.
3. The amounts of the intermetallic compounds generally decrease with increasing of the milling time.
4. Two opposite parameter will affect the transition temperatures: (1) the refinement of the powder particles, and (2) the stored energy in powders that cause faster recovery, recrystallization, and grain growth.

5. ACKNOWLEDGMENTS

The authors want to acknowledge the financial support of Sharif University of Technology. They also want to thank Mr. Daneshmaslak and Mr. Ahmadiyan for their assistance in milling and XRD tests.

6. REFERENCES

1. Benjamin, J.S.; Volin, T.E. The mechanical alloying. *Metallurgical Transactions* **1974**, *5*, 1929–1934.
2. Battezzati, L.; Cocco, G.; Schiffini, L.; Enzo, S. Thermal properties of mechanically alloyed Ni50Ti50 powders. *Journal of Materials Science and Engineering* **1988**, *97*, 121–124.
3. Stoloff, N.S.; Liu C. T.; Deevi, S.C. Emerging applications of intermetallics. *Intermetallics* **2000**, *8*, 1313–1320.
4. Westbrook, J.H.; Fleischer, R. L. *Intermetallic Compound: Structural Applications*; John Wiley and Sons: New York, 2000; 17–47.

5. Massalski, T. *Binary Alloy Phase Diagrams*; Murray, J.L., Bennett, L.H., Baker, H., Eds.; ASM, Metals Park: OH, 1986; 2847.
6. Ishida, A.; Sato, M.; Takei, A.; Nomura, K.; Miyazaki, S. Effect of aging on Shape memory behavior of Ti-51.3 at pct Ni thin films. *Metallurgical and Materials Transactions A* **1996**, *27A*, 3753–3759.
7. Lopez, H.F.; Salinas-Rodriguez, A.; Rodriguez-Galicia, J.L. Microstructural aspects of precipitation in a Ti-rich Ni–Ti alloy. *Scripta Materialia* **1996**, *34* (4), 659–664.
8. Comstock, R.J.; Buchheit, T.E.; Somerday, M.; Wert, J. A. Modeling the transactions stress of constrained shape memory alloy single crystals. *Acta Materialia* **1996**, *44* (9), 3505–3514.
9. Miyazaki, S.; Kurooka, S.; Ishida, A.; Nishida, M. Effect of heat-treatment on deformation behavior associated with R-phase and martensitic transformations in Ti-Ni thin films. *Transactions of the Materials Research Society of Japan* **1994**, *18B*, 1041–1044.
10. Miyazaki, S.; Otsuka, K.; Wayman, K. Morphological changes associated with the R-phase and martensitic transformations in Ti-Ni single crystals. *ISIJ International* **1989**, *29* (5), 423–429.
11. Nishida, M.; Honma, T. All-round shape memory effect In Ni-rich TiNi alloys generated by constrained aging. *Scripta Metallurgica* **1984**, *18*, 1295–1298.
12. Mellor, B.G.; Guilemany, J.M. Stabilized stress induced martensite—its application in two way shape memory training processes. *Scripta Metallurgica et Materialia* **1990**, *24*, 241–245.
13. Okamoto, Y.; Hamanaka, H.; Miura, F.; Tamura, H.; Horikawa, H. Reversible changes in yield stress and transformation temperature of a NiTi alloy by alternate heat treatments. *Scripta Metallurgica* **1988**, *22*, 517–520.
14. Wayman, C.M.; Duering, T.W. *An Introduction to Martensite and Shape Memory, Engineering Aspects of Shape Memory Alloys*, Shape Memory Alloy Technology Conference, Michigan State University, August 15–17, 1988; Butterworth-Heinemann: London, 1990; 3–19.
15. Tang, Weijia. Thermodynamic Study of the low-temperature phase B19 and the martensitic transformation in near-equiatomic Ti-Ni shape memory alloys. *Metallurgical Transactions A* **1997**, *23A*, 537–544.
16. Otsuka, K.; Ren, X. Martensitic Transformations in nonferrous shape memory alloys. *Materials Science and Engineering* **1999**, *30A*, 89–105.
17. Todoroki, T.; Tamura, H. Effect of heat treatment after cold working on the phase transformation in TiNi alloy. *Transactions of Japan Institute of Metals* **1987**, *28* (2), 83–94.
18. Honma, T.; Nishida, M.; Yamauchi, K. Ti–Ni Alloy Articles Having a Property of Reversible Shape Memory and a Method of Making the Same. US Patent 4,707,196, November 1987.
19. Zarandi, F.M.H.; Sadrnezhaad, K. Thermomechanical study of combustion synthesized Ti-Ni shape memory alloy. *Materials and Manufacturing Processes* **1997**, *12* (6), 1093–1105.
20. Sadrnezhaad, K.; Mashhadi, F.; Sharghi, R. Heat treatment of Ni-Ti alloy for improvement of shape memory effect. *Materials and Manufacturing Processes* **1997**, *12* (1), 107–115.

21. Igharo, M.; Wood, J.V. Compaction and sintering phenomena in Titanium-Nickel shape memory alloys. *Powder Metallurgy* **1985**, *28* (3), 131–139.
22. Takasaki, A. Mechanical alloying of the Ni-Ti system. *Physic Stat. Sol.* **1998**, *169*, 183–191.
23. Rozner, A.G.; Heintzelman, E.F.; Buehler, W.J.; Gilfrich, J.V. Effect of addition of oxygen, nitrogen and hydrogen on microstructure and hardness of cast TiNi intermetallic compound. *Transactions of the ASM* **1965**, *58*, 415–418.
24. Green, S.M.; Grant, D.M.; Kelly, N.R. Powder metallurgical processing of Ni–Ti shape memory alloy. *Powder Metallurgy* **1997**, *40* (1), 43–47.
25. Igharo, M.; Wood, J.V. Compaction and sintering phenomena in Titanium-Nickel shape memory alloys. *Powder Metallurgy* **1985**, *28* (3), 131–139.
26. Li, Bing-Yun; Rong, Li-Jian; Li, Yi-Yi; Gjunter, V. E. A recent development in producing porous Ni–Ti shape memory alloys. *Intermetallics* **2000**, *8*, 881–884.
27. Chank, Y.; Berger, S.; Weiss Brook-Levinson, B. Z. Solid state amorphization by mechanical alloying—an atomistic model. *Acta Materialia* **1994**, *42* (11), 3679–3685.
28. Rydin, R.W.; Maurice, D.; Courtney, T.H. Milling Dynamics: Part I. Attritor dynamics: Results of a cinematographic study. *Metallurgical Transactions A* **1993**, *24A*, 175–185.
29. Cook, T.M.; Courtney, T.H. The effect of ball size distribution on attritor efficiency, *Metallurgical and Materials Transactions A* **1995**, *26A*, 2389–2397.
30. Wang, K.Y.; Shen, T.D.; Wang, J.T.; Quan, M.X. Characteristics of the mechanically alloyed Ni 60 Ti 40 amorphous powders during mechanical milling in different atmospheres. *Journal of Materials Science* **1993**, *28*, 6474–6478.
31. Maurice, D.; Courtney, T.H. Milling dynamics: part II, Dynamics of a SPEX mill and a one dimensional milling. *Metallurgical and Materials Transactions A* **1996**, *27A*, 1973–1979.
32. Pabi, S.K.; Das, D.; Mahapatra, T.K.; Manna, I. Mathematical Modeling of the mechanical alloying kinetics. *Acta Materialia* **1998**, *46* (10), 3501–3510.
33. Cohen, M. Martensitic nucleation—revisited. *Materials Transactions Journal*, **1992**, *33* (3), 178–181.
34. Gordon, D. *Powder Metallurgy, the Process and Its Products*; McGraw Hill Publisher, 1990.
35. Bastin, G.F.; Rieck, G.D. Diffusion in Ni-Ti systems: Part I. *Metallurgical Transactions A* **1974**, *5A*, 1817–1826.
36. Germani, R.M. Phase diagram in liquid phase sintering treatments. *JOM* **1986**, 26–29.
37. Mirabolghasemi, S.H.; Selahi, A.; Haeri, E.; Sadrnezhaad, S.K. Thirteenth Iranian Foundrymen Society Conference, Tehran, Iran, 2001, 237–244; [In Persian].